

Granular gases under resetting

Anna S. Bodrova

Moscow Institute of Electronics and Mathematics, HSE University, 123458, Moscow, Russia

Aleksei V. Chechkin

*Institute of Physics and Astronomy, University of Potsdam, 14476 Potsdam, Germany and
Faculty of Pure and Applied Mathematics, Wrocław University of
Science and Technology, Wyspińskiego 27, Wrocław, 50-370, Poland*

Awadhesh Kumar Dubey

Department of Pure and Applied Physics, Guru Ghasidas Vishwavidyalaya, Koni, Bilaspur-495009 Chhattisgarh, India.

(Dated: October 17, 2024)

We investigate the granular temperatures in force-free granular gases under exponential resetting. When a resetting event occurs, the granular temperature attains its initial value, whereas it decreases because of the inelastic collisions between the resetting events. We develop a theory and perform computer simulations for granular gas cooling in the presence of Poissonian resetting events. We also investigate the probability density function to quantify the distribution of granular temperatures. Our theory may help understand the behavior of non-periodically driven granular systems.

I. INTRODUCTION

A process with resetting breaks at a certain point and starts anew. Resetting has been widely studied recently and has numerous applications [1, 2]. This significantly accelerates the search processes [3–5] and improves the efficiency of computer algorithms [6, 7]. The resetting processes have been observed in various fields. In biology, resetting occurs in enzyme-catalyzed reactions, described in terms of Michaelis-Menten kinetics [8–10], transcription [11], and mobility of animals [12]. In economic society models, resetting may represent a loss of wealth due to catastrophic events [13]. Geometric Brownian motion with stochastic resetting can be used to describe income dynamics [14, 15]. Resetting may represent eye movements while viewing and recognizing the patterns [16, 17].

In the first study, resetting was considered for particles that exhibited overdamped Brownian motion [18, 19]. Subsequently, many other processes with resetting have been investigated, such as underdamped Brownian motion [20, 21] the Ornstein-Uhlenbeck process [22, 23], continuous-time random walks [24–29], Lévy flights [30, 31], Lévy walks [32], heterogeneous diffusion processes [33, 34], fractional Brownian motion [34], geometric Brownian motion [35], scaled Brownian motion [36, 37], and resetting on networks [38]. Initially, the resetting process was considered as a jump to the starting point. Later, other types of return processes were considered, such as partial resetting [39, 40], return at constant velocity [5, 41–46], and under the action of an external potential [47–49]. The latter phenomenon was observed in experiments [50–52]. Most investigations have dealt with the resetting of coordinates. However, the resetting of other quantities has also been considered, such as the diffusion coefficient in scaled Brownian motion [36, 37] and velocity in underdamped Brownian motion [20, 21],

In this study, we investigate the resetting in granu-

lar systems. There are numerous examples of granular systems, such as stones and sand in the building industry; grains, sugar, salt, and cereals in the food industry; and different kinds of powders in chemical and cosmetic production [53–56]. Granular materials consist of macroscopic solid particles but can also exhibit behavior similar to that of conventional phases of matter. They can flow like liquids down an incline and be in a gaseous state, when the particles move at high velocities, and the typical distance between granular particles exceeds their size.

Numerous examples of granular gases include dust devils, large interstellar dust clouds [59], protoplanetary discs, planetary rings [60–62], and asteroids [63]. There are several different possibilities for simulating granular systems in computer experiments [83], such as Monte Carlo (MC) and molecular dynamics (MD). The former allows for more rapid simulations of large systems, whereas the latter resembles the properties of real systems.

Granular gases have many similarities with molecular gases [56–58]. However, the major difference between them is the dissipative collisions, where part of the kinetic energy of the granular gases is lost [57]. The motion of the particles slows down, and the system homogeneously cools according to Haff's law [80]. Although clustering and vortex formation can be observed at the later stages of the evolution of granular systems [57], the homogeneous state may persist long enough even for a polydisperse system [81]. Although granular systems may be highly polydisperse [82], we restrict our consideration to three-dimensional unicomponent granular gases.

To maintain a gaseous state, energy should be supplied to the system. There are different possibilities for providing energy supply to granular systems: vibrating [64, 65] or rotating [66] walls, external electrostatic [67] or magnetic forces [68–71].

The driving of granular gases is often described in theory and computer simulations in terms of uniform heating

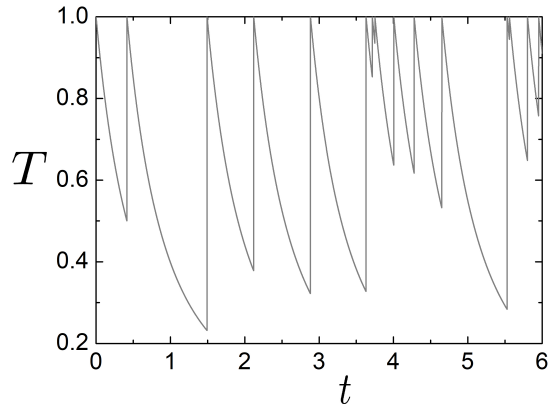


FIG. 1. A typical evolution of granular temperature $T(t)$ in granular systems with exponential resetting. The resetting rate $r = 2$, the characteristic time of the granular temperature decay $\tau_0 = 1$, the initial granular temperature $T_0 = 1$.

[72–75] or heating through the boundaries [76, 77]. The heating events may also occur as rare but powerful energy injections into a single randomly selected particle [78, 79]. In addition, particles may be reenergized such that their velocities are drawn from a Maxwellian distribution with a typical energy proportional to the system size [79]. Velocity distribution functions have been studied for various driving mechanisms. It has been shown that the velocity distribution of granular gases is governed by the heating-dissipation rate, which is given as the ratio between the average number of heating events and the average number of collisions [76, 77]. However, the quantitative dependence of the most important macroscopic parameters, such as granular temperature, on the ratio between the average number of heating events and average number of collisions has not been derived before. This dependence may be universal in systems with different driving mechanisms.

We describe rare heating events within the framework of resetting of granular temperatures. We consider Poissonian resetting, which means that the resetting event may occur with equal probability at any given time. During the instantaneous resetting event, the granular temperature attains its initial value, T_0 . Between the resetting events, the system evolves force-free by itself and cools homogeneously according to Haff’s law [80].

We proceed as follows. In Section II, we briefly review the evolution of the force-free granular gases. In Section III, we present our theory of the Poissonian resetting of granular gases and study the probability density function (PDF) of the granular temperatures and its moments. We discuss event-driven numerical simulations and compare them with theory in Sec. IV. Finally, we present our conclusions in Sec. V.

II. HAFF’S LAW

The granular temperature is one of the most important parameters in the description of granular gases. This is defined in terms of the mean kinetic energy [57]

$$\frac{3}{2}nT(t) = \frac{m\langle v^2 \rangle}{2} = \int d\mathbf{v} f(\mathbf{v}, t) \frac{mv^2}{2}. \quad (1)$$

Here, m is the mass of the granular particle, v corresponds to its velocity, n is the number density of particles in the granular gas, and $f(\mathbf{v}, t)$ is the velocity distribution function, which is assumed to be Maxwellian for simplicity, despite the slight deviations from the Maxwellian form obtained in both theory [84–91] and experiments [92]. Owing to the dissipative collisions, the granular temperature in the granular gas gradually decreases. The evolution of granular temperature obeys the following differential equation [57]:

$$\frac{dT(t)}{dt} = -T(t)\xi(t). \quad (2)$$

Here the cooling rate $\xi(t)$ is equal to [57]

$$\xi(t) = \frac{4}{3}(1 - \varepsilon^2)n\sigma^2\sqrt{\frac{\pi T}{m}}, \quad (3)$$

where, σ is the diameter of the granular particles, and the restitution coefficient ε quantifies the dissipative losses during the collision of granular particles as follows [56, 57]:

$$\varepsilon = \left| \frac{(\mathbf{v}'_{ki} \cdot \mathbf{e})}{(\mathbf{v}_{ki} \cdot \mathbf{e})} \right|. \quad (4)$$

Here, $\mathbf{v}_{ki} = \mathbf{v}_k - \mathbf{v}_i$ and $\mathbf{v}'_{ki} = \mathbf{v}'_k - \mathbf{v}'_i$ are the relative velocities before and after a collision, respectively, and \mathbf{e} is a unit vector directed along the inter-center vector at the collision instant. For simplicity, the restitution coefficient is often assumed constant [57]. It is easy to implement in analytical calculations, and can be considered a basic reference model. The post-collision velocities \mathbf{v}'_k and \mathbf{v}'_i are related to the pre-collision velocities \mathbf{v}_k and \mathbf{v}_i as follows [57]:

$$\mathbf{v}'_{k/i} = \mathbf{v}_{k/i} \mp \frac{1 + \varepsilon}{2}(\mathbf{v}_{ki} \cdot \mathbf{e})\mathbf{e}. \quad (5)$$

Differential equation (Eq. 2) with the cooling rate (Eq. 3) can be solved explicitly, and the temperature obeys Haff’s law [80]

$$T(t) = T_0 \left(1 + \frac{t}{\tau_0} \right)^{-2}, \quad (6)$$

where $T_0 = T(0)$ is the initial granular temperature. The inverse temperature relaxation time is equal to half the cooling rate at the initial time:

$$\tau_0^{-1} = \xi(0)/2. \quad (7)$$

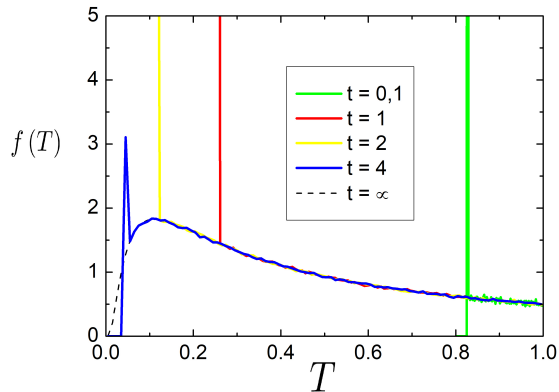


FIG. 2. Evolution of the probability density function of granular temperatures $f(T, t)$ (Eq. 13), $\tilde{r} = 1$. The peaks may be obtained by introducing the corresponding times into the Haff's law (Eq. 6). Solid lines correspond to results of MC simulations, dashed line - to theory at long times, $t \rightarrow \infty$ (Eq. 22).

III. THEORY

A. Poissonian resetting

We assume that resetting events occur according to Poisson process [93] with a constant rate r . Thus, the average time between resetting events is equal to $1/r$. The probability $r dt$ for the resetting event to occur during the time interval $(t, t + dt)$ does not depend on time t and depends only on the time interval dt . The waiting time distribution between resetting events is

$$\psi(t) = r e^{-rt}. \quad (8)$$

The survival probability $\Psi(t)$ is defined as the probability that no resetting event occurs between zero and t ,

$$\Psi(t) = 1 - \int_0^t \psi(t') dt' = e^{-rt}. \quad (9)$$

We perform computer simulations using both event-driven MD simulations (described in Section IV) and simple MC simulations. In the latter, the granular temperature evolves initially according to Haff's law (Eq. 6). If the resetting event takes place at a constant rate r , the granular temperature takes the initial value $T_0 = 1$. Subsequently, it starts to decrease again. The typical evolution of a granular system with a resetting rate $r = 0.1$ is shown in Fig. 1.

B. Probability density function

Let us consider evolution of a granular temperature with an arbitrary power-law constant a

$$T(t) = T_0 \left(1 + \frac{t}{\tau_0}\right)^{-a}. \quad (10)$$

The power-law constant a may vary for different granular cooling scenarios, for example in the presence of clustering [94]. For the viscoelastic granular gas model $a = 5/3$ [57, 87, 90].

The probability density function (PDF) $f_0(T)$ of the granular temperature distribution without resetting has the form of a Dirac delta-function:

$$f_0(T, t) = \delta\left(T - T_0 \left(1 + \frac{t}{\tau_0}\right)^{-a}\right) \quad (11)$$

The probability density function (PDF) with resetting can be obtained according to [1]:

$$f(T, t) = f_0(T, t) e^{-rt} + r \int_0^t f_0(T, \tau) e^{-r\tau} d\tau. \quad (12)$$

The first term accounts for the realizations where no resetting occurs up to observation time t . In this case the evolution of the granular temperature is determined by the generalized form of Haff's law (Eq. 10), and the PDF takes the form of a Dirac delta-function. The second term accounts for the case in which the last resetting event occurs at time $t - \tau$, after which no resetting occurs between $t - \tau$ and t with probability $\Psi(\tau)$ (Eq. 9). The PDF value is determined by the time interval τ passed from the last resetting event owing to the memory loss. Introducing Eq. (11) into Eq. (12) and performing the integration, we find that the PDF has the form

$$f(T, t) = \delta\left(T - T_0 \left(1 + \frac{t}{\tau_0}\right)^{-a}\right) e^{-rt} + \frac{\tilde{r}}{a T_0} \left(\frac{T_0}{T}\right)^{1+1/a} \times \exp\left(\tilde{r} \left(1 - (T_0/T)^{1/a}\right)\right) \Theta\left(T - T_0 \left(1 + \frac{t}{\tau_0}\right)^{-a}\right) \quad (13)$$

for $0 < T \leq T_0$ and zero otherwise. Here, we introduced the parameter $\tilde{r} = r\tau_0$ as the ratio between the characteristic temperature relaxation time and average time $1/r$ between resetting events, and $\Theta(x)$ is the Heaviside step function. At long times $t \gg 1/r$ the probability that no resetting events have occurred tends to zero, and the first term in Eq. (13) can be neglected. By setting $t \rightarrow \infty$, we obtain the steady-state value of the PDF

$$f(T, t) = \frac{\tilde{r}}{a T_0} \left(\frac{T_0}{T}\right)^{1+1/a} \exp\left(\tilde{r} \left(1 - (T_0/T)^{1/a}\right)\right). \quad (14)$$

In such a way, the PDF of reciprocal reduced granular temperatures T_0/T has the form of Gamma distribution. The mean granular temperature may be obtained using the PDF (Eq. 13):

$$\langle T(t) \rangle = \int_0^{T_0} f(T, t) T dT = T_0 e^{-rt} \left(1 + \frac{t}{\tau_0} \right)^{-a} + T_0 \tilde{r} e^{\tilde{r}} \left(E_a(\tilde{r}) - \left(1 + \frac{t}{\tau_0} \right)^{1-a} E_a \left(\tilde{r} \left(1 + \frac{t}{\tau_0} \right) \right) \right) \quad (15)$$

with $E_a(z)$ being the generalized integro-exponential function [95]:

$$E_a(z) = \int_1^\infty \frac{e^{-zt}}{t^a} dt. \quad (16)$$

In the long time limit $t \rightarrow \infty$ this value tends to

$$T_c = T_0 \tilde{r} e^{\tilde{r}} E_a(\tilde{r}). \quad (17)$$

The moments of granular temperatures can be obtained analogously

$$\langle T^\beta(t) \rangle = T_0^\beta e^{-rt} \left(1 + \frac{t}{\tau_0} \right)^{-a\beta} + T_0^\beta \tilde{r} e^{\tilde{r}} \left(E_{a\beta}(\tilde{r}) - \left(1 + \frac{t}{\tau_0} \right)^{1-a\beta} E_{a\beta} \left(\tilde{r} \left(1 + \frac{t}{\tau_0} \right) \right) \right). \quad (18)$$

In the long-time limit $t \rightarrow \infty$

$$\langle T^\beta \rangle = T_0^\beta \tilde{r} e^{\tilde{r}} E_{a\beta}(\tilde{r}) \quad (19)$$

and the variance attains the form

$$\sigma^2(T) = \langle T^2 \rangle - \langle T \rangle^2 = T_0^2 \tilde{r} e^{\tilde{r}} (E_{2a}(\tilde{r}) - \tilde{r} e^{\tilde{r}} E_a^2(\tilde{r})). \quad (20)$$

C. Constant restitution coefficient

The PDF (Eq. 13) in the case of a constant restitution coefficient ($a = 2$) becomes equal to

$$f(T, t) = \delta \left(T - T_0 \left(1 + \frac{t}{\tau_0} \right)^{-2} \right) e^{-rt} + \quad (21)$$

$$\frac{\tilde{r}}{2T} \sqrt{\frac{T_0}{T}} e^{\tilde{r}(1-\sqrt{T_0/T})} \Theta(T_0 - T) \Theta \left(T - T_0 \left(1 + \frac{t}{\tau_0} \right)^{-2} \right) \quad (22)$$

The evolution of the PDF (Eq. 21) can also be obtained by simple MC simulations of a granular system with resetting. The simulation for $N = 10^6$ different systems was performed, and the PDFs at different time moments are shown in Fig. 2. The peak shifts towards smaller

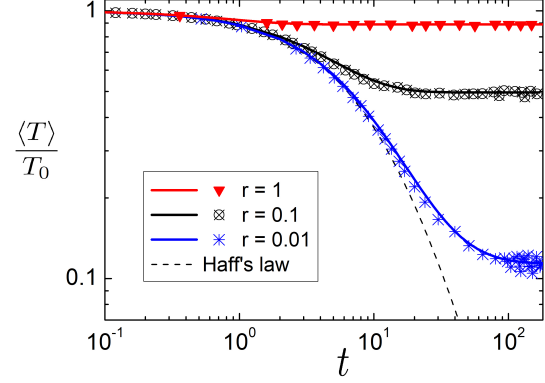


FIG. 3. Event-driven simulations of the time evolution of the granular temperature $T(t)$ in comparison with the theory. The characteristic time of the granular temperature decay $\tau_0 = 15.3$. Dashed line shows the evolution of a granular temperature of a force-free granular system without resetting according to the Haff's law. Lines correspond to analytical results (Eq. 24) and symbols correspond to results of event-driven simulations.

granular temperatures over time and eventually disappears. The steady-state value of the PDF can be obtained in the long time limit $t \rightarrow \infty$

$$f(T) = \frac{\tilde{r}}{2T} \sqrt{\frac{T_0}{T}} e^{\tilde{r}(1-\sqrt{T_0/T})} \Theta(T_0 - T) \Theta(T). \quad (22)$$

This expression is depicted by the dashed line in Fig. 2. The mean granular temperature can be derived from the PDF using Eq. (15) or the expression

$$\langle T(t) \rangle = T_0 \left(1 + \frac{t}{\tau_0} \right)^{-2} e^{-rt} + r \int_0^t T_0 \left(1 + \frac{\tau}{\tau_0} \right)^{-2} e^{-r\tau} d\tau. \quad (23)$$

The direct integration of this equation yields

$$\langle T(t) \rangle = T_0 \left[\left(1 + \frac{t}{\tau_0} \right)^{-2} e^{-rt} + \tilde{r} - \tilde{r} e^{-rt} \left(1 + \frac{t}{\tau_0} \right)^{-1} + \tilde{r}^2 e^{\tilde{r}} \left(\text{Ei}(-\tilde{r}) - \text{Ei} \left(-\tilde{r} \left(1 + \frac{t}{\tau_0} \right) \right) \right) \right], \quad (24)$$

where $\text{Ei}(z)$ is exponential integral function [96]:

$$\text{Ei}(z) = - \int_{-z}^\infty \frac{e^{-t}}{t} dt. \quad (25)$$

Eq. (24) may be also obtained by integrating Eq. (15) by parts. The constant value of the granular temperature has the form

$$T_c = \tilde{r} T_0 (1 - \tilde{r} \Gamma(0, \tilde{r}) e^{\tilde{r}}), \quad (26)$$

where $\Gamma(0, \tilde{r})$ is the incomplete gamma function. At $\tilde{r} \rightarrow 0$ the constant average granular temperature scales as

$$T_c = T_0 (\tilde{r} + (\gamma + \log \tilde{r}) \tilde{r}^2 + o(\tilde{r}^2)), \quad (27)$$

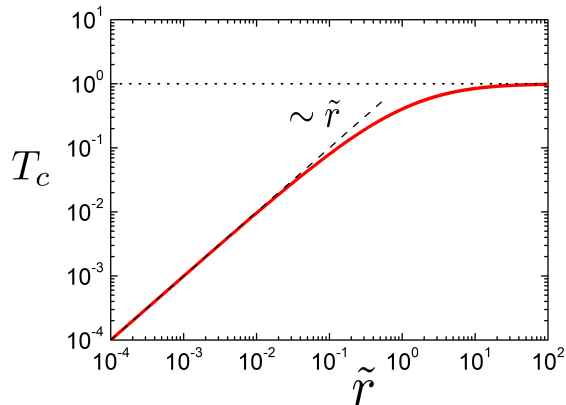


FIG. 4. Dependence of the steady-state value of granular temperature T_c on the ratio between resetting and cooling rates $\tilde{r} = 2r/\xi(0)$, Eq. (17). Thick red line corresponds to a granular gas of particles, colliding with a constant restitution coefficient. The dashed line shows linear dependence at short times, $T_c \sim \tilde{r}$. At large \tilde{r} the average granular temperature tends to the initial value $T_0 = 1$, depicted with a dotted line.

where γ is Euler's constant. At $\tilde{r} \rightarrow \infty$ Eq. (26) becomes

$$T_c = T_0 \left(1 - \frac{2}{\tilde{r}} + \frac{6}{\tilde{r}^2} + o\left(\frac{1}{\tilde{r}^2}\right) \right). \quad (28)$$

The evolution of the mean granular temperature $\langle T(t) \rangle$ according to Eq. (24) is shown in Fig. 3. At the beginning of the evolution, it decreases according to Haff's law and then reaches a constant value T_c : At low resetting rates $r \rightarrow 0$ the mean time between the resetting events tends to infinity and the granular temperature evolves freely according to Haff's law (Eq. 6). If the resetting events are very frequent, and the resetting rate is much larger than the cooling rate, $r \gg \tau_0^{-1}$, the temperature remains constant, close to its initial value, $T \simeq T_0$.

The dependence of steady-state granular temperature T_c on \tilde{r} is shown in Fig. 4. At low resetting rates compared with the cooling rates, $\tilde{r} \ll 1$, it increases linearly according to Eq. (27), and at high reduced resetting rates $\tilde{r} \gg 1$, it remains close to the initial value $T_0 = 1$. In the latter case the temperature was essentially reduced between the subsequent resetting events.

The variance of the granular temperature in the steady state for granular gas with a constant restitution coefficient may be written as according to Eq. (20):

$$\sigma^2(T) = T_0^2 \tilde{r} e^{\tilde{r}} \left(E_4(\tilde{r}) - \tilde{r} e^{\tilde{r}} E_2^2(\tilde{r}) \right). \quad (29)$$

The dependence of the variance of granular temperatures on the reduced resetting rate \tilde{r} is shown in Fig. 5. At $\tilde{r} \rightarrow 0$ the variance scales according to

$$\sigma^2(T) = T_0^2 \left(\frac{1}{3} \tilde{r} - \frac{7}{6} \tilde{r}^2 + o(\tilde{r}^2) \right). \quad (30)$$

At low resetting rates, the variance increases linearly, as depicted by the dashed line in Fig. 5. Subsequently, it

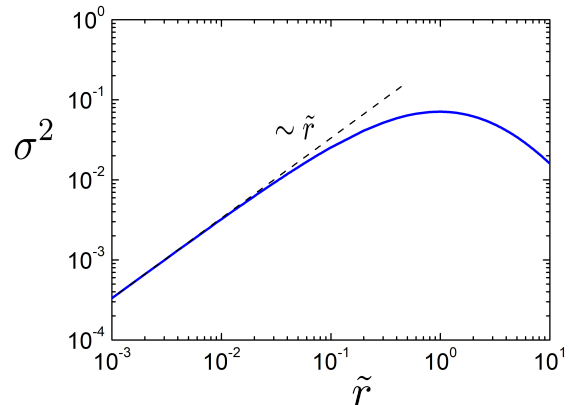


FIG. 5. Dependence of variance of granular temperature $\sigma^2(T)$ on the ratio between resetting and cooling rates $\tilde{r} = 2r/\xi(0)$, Eq. (29). The dashed line shows linear dependence at short times, $\sigma^2(T) \sim \tilde{r}$.

reaches its maximum value and then decreases. This has a clear physical explanation: at very low and very high resetting rates, the value of the granular temperature is strictly determined. In the former case, it decreases according to Haff's law, whereas in the latter case, it tends to a constant value. The most diverse behavior appears in the system at an intermediate resetting rate $\tilde{r} \simeq 1$.

IV. EVENT-DRIVEN SIMULATIONS

We perform event-driven MD simulations [83] of a dilute force free three dimensional granular gas of smooth particles colliding with a constant restitution coefficient ϵ . We consider identical grains modeled as hard spheres of equal mass ($m = 1$) and diameter ($\sigma = 1$). In our simulations we undertake a system of $N_{\text{par}} = 10^5$ particles in a three-dimensional cubic box with edge $L = 158$ corresponding to a number density $n \approx 0.025$. This number density is small and validates the assumption of binary collisions. The particles move freely between two successive collisions. After each collision the velocities of the particles are updated according to the collision rules given by Eqs. (5).

The simulation starts by randomly placing the particles in the box with periodic boundary conditions. The particles are assigned velocity vectors of equal magnitudes but in random directions. We ensure that the initial total momentum $\sum_i m \mathbf{v}_i(0)$ was zero with high accuracy. Initially, we let the system relax to the Maxwellian velocity distribution by allowing particles to collide elastically ($\epsilon = 1$). This takes place in a few collisions per particle resulting into a system of homogeneous granular gas with Maxwellian velocity distribution and we consider this configuration (positions and velocities) as system's initial condition. Thereafter, we assign $\epsilon = 0.9$ and let the system evolve with time via inelastic collisions.

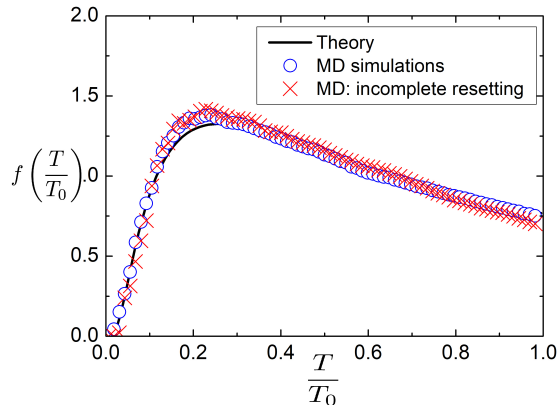


FIG. 6. Probability density function of granular temperatures $f(T)$ for $\tau_0 = 15.3$, $r = 0.1$, $t = 100$. Symbols denote the results of event-driven simulations for both complete and incomplete resetting, line corresponds to the analytical form of the steady-state distribution of granular temperatures (Eq. 22).

We confirm that the system follows Haff's law and remains in a homogeneous cooling state (HCS) throughout the simulation. We have taken the initial granular temperature $T(0) = 400/3$ and have obtained the results by averaging over 800 independent initial conditions. The granular temperature relaxation time (Eq. 7) becomes equal to $\tau_0 = 15.3$.

The resetting occurs by assigning initial velocities to all the constituent particles at randomly selected times for which the waiting time distribution is given by Eq. (8). The system regains its initial temperature $T(0) = 400/3$ after resetting. The typical evolution of a granular system with a resetting rate $r = 2$ is shown in Fig. 1. The evolution of the mean granular temperature $\langle T(t) \rangle$, obtained in the simulations, is in good agreement with the theory, Eq. (24) (Fig. 3). A comparison of the granular temperature PDF, obtained in the simulations with the theoretical value is shown in Fig. 6 and excellent agreement is again observed.

In addition, we consider the case of the incomplete resetting. We randomly choose half of the particles and scale their velocities such that the total kinetic energy (or granular temperature) regains its initial value. Thus, if the velocity of any i^{th} particle from the randomly selected

ones is \mathbf{v}_i then the scaled velocity

$$\mathbf{v}_i^s = \alpha * \mathbf{v}_i \quad (31)$$

where the scaling factor

$$\alpha = \sqrt{\frac{T(0) - T_r(t)}{T_c(t)}} \quad (32)$$

Here, $T_c(t)$ is the temperature of the chosen half of the particles and $T_r(t)$ is the temperature of the rest half. The comparison in Fig. 6 shows that the incompleteness of resetting does not affect essentially the steady-state distribution of granular temperature. This observation confirms universality of our theory that can be applied to different resetting protocols.

V. CONCLUSIONS

Granular systems with resets were investigated. We assume that at the resetting event, the granular temperature is instantly reset to the initial value. This may occur when the container with the granular material is shaken from time to time, a magnetic force is applied, or if energy is instantly inserted into the granular system in a different manner. The mean granular temperature was derived analytically and calculated in terms of both event-driven and Monte Carlo simulations. After a certain relaxation time it tends to a constant value, which decreases with increasing the average interval between resetting events. The variance in the granular temperature reaches its maximum at intermediate resetting rates, tending to zero for both vanishing and extremely large resetting rates. Thus, the granular temperature of the driven granular medium may be controlled by the resetting rate. Our results may be helpful for understanding non-periodically driven granular systems.

VI. ACKNOWLEDGEMENT

A.S.B. thanks Erez Aghion for the fruitful discussions.

-
- [1] M. R Evans, S. N. Majumdar, and G. Schehr, *J. Phys. A* **53**, 193001 (2020).
 - [2] S. Gupta and A. M. Jayannavar, *Front. Phys.* **10**, 789097 (2022).
 - [3] A.V. Chechkin, I.M. Sokolov, *Phys. Rev. Lett.* **121**, 050601 (2018).
 - [4] A. Pal and S. Reuveni, *Phys. Rev. Lett.* **118**, 030603 (2017).
 - [5] A. Pal, L. Kuśmierz, S. Reuveni, *Phys. Rev. Research* **2**, 043174 (2020).
 - [6] A. Montanari and R. Zecchina, *Phys. Rev. Lett.* **88**, 178701 (2002).
 - [7] J. H. Lorenz, *PLoS One*, **11** 043202 (2016).

- [8] S. Reuveni, M. Urbach, and J. Klafter, *Proc. Natl. Akad. Sci. U.S.A.* **111**, 4391 (2014).
- [9] T. Rotbart, S. Reuveni, M. Urbakh, *Phys. Rev. E* **92**, 060101(R) (2015).
- [10] T. Robin, S. Reuveni, M. Urbakh, *Nat. Commun.* **9**, 779 (2018).
- [11] É. Roldán, A. Lisica, D. Sánchez-Taltavull, and S.W. Grill, *Phys. Rev. E* **93**, 062411 (2016).
- [12] D. Boyer, C. Solis-Salas, *Phys. Rev. Lett.* **112**, 240601 (2014).
- [13] I. Santra, *Europhys. Lett.* **137**, 52001 (2022).
- [14] P. Jolakoski, A. Pal, T. Sandev, L. Kocarev, R. Metzler, V. Stojkoski, *Chaos, Solitons & Fractals* **175**, 113921 (2023).
- [15] V. Stojkoski, P. Jolakoski, A. Pal, T. Sandev, L. Kocarev, and R. Metzler, *Phil. Trans. R. Soc. A* **380** 20210157 (2022).
- [16] D. Noton, L. Stark, *Vis Res* **11** 929 (1971).
- [17] M.P. Eckstein, *J. Vis.* **11** 14 (2011).
- [18] M. R. Evans and S. N. Majumdar, *Phys. Rev. Lett.* **106**, 160601 (2011).
- [19] S. N. Majumdar, S. Sabhapandit, G. Schehr, *Phys. Rev. E* **91**, 052131 (2015).
- [20] D. Gupta, *J. Stat. Mech.* 033212 (2019).
- [21] K. S. Olsen and H. Löwen *J. Stat. Mech.* 033210 (2024).
- [22] A. Pal, *Phys. Rev. E* **91**, 012113 (2015).
- [23] P. Trajanovski, P. Jolakoski, K. Zelenkovski, A. Iomin, L. Kocarev, and T. Sandev, *Phys. Rev. E* **107**, 054129 (2023)
- [24] A.S. Bodrova, I.M. Sokolov, *Phys. Rev. E* **101**, 062117 (2020).
- [25] M. Montero and J. Villarroel, *Phys. Rev. E* **87**, 012116 (2013).
- [26] V. Méndez and D. Campos, *Phys. Rev. E* **93**, 022106 (2016).
- [27] V.P. Shkilev, *Phys. Rev. E* **96**, 012126 (2017).
- [28] M. Montero, A. Mas-Puigdellosas, J. Villarroel. *Eur. Phys. J. B* **90**, 176 (2017).
- [29] L. Kuśmierz, E. Gudowska-Nowak, *Phys. Rev. E* **99**, 052116 (2019).
- [30] L. Kuśmierz, S. N. Majumdar, S. Sabhapandit, and G. Schehr, *Phys. Rev. Lett.* **113**, 220602 (2014).
- [31] L. Kuśmierz, E. Gudowska-Nowak, *Phys. Rev. E* **92**, 052127 (2015).
- [32] T. Zhou, P. Xu, W. Deng, *Phys. Rev. Research* **2**, 013103.
- [33] T. Sandev, V. Domazetoski, L. Kocarev, R. Metzler, and A. Chechkin, *J. Phys. A: Math. Theor.* **55** 074003 (2022)
- [34] W. Wang, A.G. Cherstvy, H. Kantz, R. Metzler, and I.M. Sokolov, *Phys. Rev. E* **104** 024105 (2021)
- [35] D. Vinod, A.G. Cherstvy, W. Wang, R. Metzler, and I.M. Sokolov, *Phys. Rev. E* **105** L012106 (2022)
- [36] A.S. Bodrova, A.V. Chechkin, I.M. Sokolov, *Phys. Rev. E* **100**, 012120 (2019).
- [37] A.S. Bodrova, A.V. Chechkin, I.M. Sokolov, *Phys. Rev. E* **100**, 012119 (2019).
- [38] A. P. Riascos, D. Boyer, P. Herringer, and J. L. Mateos, *Phys. Rev. E* **101** 062147 (2020)
- [39] M. Dahlenburg, A. V. Chechkin, R. Schumer, and R. Metzler, *Phys. Rev. E* **103**, 052123 (2021).
- [40] C. Di Bello, A. V. Chechkin, A. K. Hartmann, Z. Palmowski, and R. Metzler, *New J. Phys.* **25**, 082002 (2023).
- [41] A.S. Bodrova, I.M. Sokolov, *Phys. Rev. E* **101**, 052130 (2020).
- [42] A.S. Bodrova, I.M. Sokolov, *Phys. Rev. E* **102**, 032129 (2020).
- [43] A. Pal, L. Kuśmierz, S. Reuveni, *New J. Phys.* **21**, 113024 (2019).
- [44] A. Pal, L. Kuśmierz, S. Reuveni, *Phys. Rev. E* **100**, 040101(R) (2019).
- [45] A. Masó-Puigdellosas, D. Campos, and V. Méndez, *Phys. Rev. E* **100**, 042104 (2019).
- [46] M. Radice, *J. Phys. A: Math. Theor.* **55**, 224002 (2022).
- [47] D. Gupta, C.A. Plata, A. Kundu, and A. Pal, *J. Phys. A: Math. Theor.* **54**, 025003 (2020).
- [48] D. Gupta, C.A. Plata, A. Pal, and A. Kundu, *J. Stat. Mech.*, 043202 (2021).
- [49] I. Santra, S. Das and S. K. Nath, *J. Phys. A: Math. Theor.* **54**, 334001 (2021).
- [50] O. Tal-Friedman, A. Pal, A. Sekhon, S. Reuveni, and Y. Roichman, *J. Phys. Chem. Lett.* **11**, 7350 (2020).
- [51] B. Besga, A. Bovon, A. Petrosyan, S. N. Majumdar, and S. Ciliberto, *Phys. Rev. Res.* **2**, 032029(R) (2020).
- [52] F. Faisant, B. Besga, A. Petrosyan, S. Ciliberto, and S. N. Majumdar, *J. Stat. Mech.* **2021**, 113203 (2021).
- [53] H. Hinrichsen, D. E. Wolf *The Physics of Granular Media*. (Berlin: Wiley, 2004).
- [54] J. Duran, *Sands, Powders and Grains*. Berlin: Springer-Verlag, (2000).
- [55] H. J. Herrmann, J.-P. Hovi and S. Luding, *Physics of Dry Granular Media*. Dordrecht: NATO ASI Series, Kluwer (1998).
- [56] H. Jaeger, S. Nagel, & R. Behringer, *Rev. Mod. Phys.* **68**, 1259 (1996).
- [57] N. V. Brilliantov, T. Pöschel, *Kinetic theory of Granular Gases*. Oxford: Oxford University Press (2004).
- [58] A. Mehta, in *Granular Physics*, Cambridge University Press (2011);
- [59] G. Winnewiser, G.C. Pelz *The physics and chemistry of interstellar molecular clouds*. Proceedings of the 2nd Cologne-Zermatt Symposium Held at Zermatt, Switzerland, Springer (1993).
- [60] R. Greenberg, A. Brahic, *Planetary rings*. University of Arizona Press, Tucson (1984).
- [61] F. G. Bridges, A. Hatzes and D. N. C. Lin, *Nature* **309**, 333 (1984).
- [62] N.V. Brilliantov, P. L. Krapivsky, A. Bodrova, F. Spahn, H. Hayakawa, V. Stadnichuk, J. Schmidt, *Proc. Natl. Acad. Sci. USA* **112**, 9536 (2015).
- [63] D. Hestroffer, P. Sánchez, L. Staron et al. *Astron. Astrophys. Rev.* **27**, 6 (2019).
- [64] R. D. Wildman and D. J. Parker, *Phys. Rev. Lett.*, **88**, 064301 (2002).
- [65] A. Prevost, D. A. Egolf and J. S. Urbach, *Phys. Rev. Lett.*, **89**, 084301 (2002).
- [66] O. Zik, D. Levine, S.G. Lipson, S. Shtrikman and J. Stavans, *Phys. Rev. Lett.*, **73**, 644 (1994).
- [67] I. S. Aranson and J. S. Olafsen, *Phys. Rev. E*, **66**, 061302 (2002).
- [68] A. Snezhko, I. S. Aranson and W.-K. Kwok, *Phys. Rev. Lett.*, **94**, 108002 (2005).
- [69] C. C. Maass, N. Isert, G. Maret and C. M. Aegerter, *Phys. Rev. Lett.*, **100**, 248001 (2008).
- [70] M. Adachi, P. Yu, and M. Sperl, *npj Microgravity* **5**, 19 (2019).
- [71] M. Adachi, M. Balter, X. Cheng, et al. *Microgravity Sci. Technol.* **33**, 11 (2021).

- [72] J. M. Montanero and A. Santos, *Granular Matter* **2**, 53 (2000).
- [73] R. Cafiero, S. Luding, *Phys. A* **280**, 142 (2000).
- [74] A. Megías, A. Santos, *Granular Matter* **21**, 49 (2019).
- [75] V.V. Prasad, R. Rajesh, *J. Stat. Phys.* **176**, 1409 (2019).
- [76] J. S. van Zon, and F. C. MacKintosh, *Phys. Rev. Lett.* **93**, 038001 (2004).
- [77] J. S. van Zon, and F. C. MacKintosh, *Phys. Rev. E* **72**, 051301 (2005).
- [78] W. Kang, J. Machta and E. Ben-Naim, *Europhys. Lett.* **91**, 34002 (2010).
- [79] E. Ben-Naim and J. Machta, *Phys. Rev. Lett.* **94**, 138001 (2005)
- [80] P. K. Haff, *J. Fluid Mech.*, **134**, 401 (1983).
- [81] H. Uecker, W.T. Kranz, T. Aspelmeier, A. Zippelius, *Phys. Rev. E* **80**, 041303 (2009).
- [82] A. S. Bodrova, *Phys. Rev. E*, **109**, 024903 (2024).
- [83] T. Pöschel and T. Schwager, *Computational Granular Dynamics*, Springer, Berlin, (2005).
- [84] A. Goldshtein and M. Shapiro, *J. Fluid Mech.* **282**, 75 (1995).
- [85] T. P. C. van Noije and M. H. Ernst, *Gran. Mat.* **1**, 57 (1998).
- [86] M. Huthmann, J. A. Orza, and R. Brito, *Gran. Mat.* **2**, 189 (2000).
- [87] N. V. Brilliantov and T. Pöschel, *Phys. Rev. E* **61**, 5573 (2000).
- [88] N. V. Brilliantov and T. Pöschel, *Europhys. Lett.* **74**, 424 (2006).
- [89] A.S. Bodrova, N.V. Brilliantov, *Physica A* **388**, 3315 (2009).
- [90] A.S. Bodrova, N.V. Brilliantov, *Mosc. Univ. Phys. Bull.* **64**, 128 (2009).
- [91] A.K. Dubey, A.S. Bodrova, S. Puri, N.V. Brilliantov, *Phys. Rev. E* **87**, 062202 (2013).
- [92] P. Yu, M. Schröter, M. Sperl, *Phys. Rev. Lett.*, **124** (20), 208007 (2020).
- [93] J. F. C. Kingman, *Poisson Processes*, Clarendon Press (1992).
- [94] P. Das, S. Puri, and M. Schwartz, *Phys. Rev. E* **94**, 032907 (2016).
- [95] M. S. Milgram, *Mathematics of computation*, **44**, 443 (1985).
- [96] M. Abramowitz and I. A. Stegun, *Handbook of Mathematical Functions* (Dover, Mineola, NY, 1965).